

# Tidal resource, turbine wake and performance modelling on the EnFAIT project

Alasdair Macleod, Andrew Watson, David Quantrell, Sam Porteous and Tom Wills

**Abstract**—Enabling Future Arrays in Tidal (EnFAIT) is an EU Horizon 2020 flagship tidal energy project. It aims to demonstrate the development, operation and decommissioning of the world's largest tidal array (six turbines), over a five-year period, to prove a cost reduction pathway for tidal energy and that it can be cost competitive with other forms of renewable energy.

The astronomical forces that produce the tide are highly predictable but estimating the energy that can be extracted from a tidal stream requires the consideration of multiple influencing factors such as seabed shape, local flow effects and array interactions. To design a tidal energy project, the impact of ambient turbulence and turbine wakes on power output and system loads must also be considered. This paper presents the work, to date, by Nova Innovation and ORE Catapult to validate a model of the world's first grid-connected tidal array.

The EnFAIT tidal array is being simulated by developing and combining three numerical models validated with field recorded data. By integrating three numerical models: a) A tidal energy resource model of Bluemull Sound, b) A tidal turbine wake and interaction model and c) a structural loads and performance model, the EnFAIT array will be simulated. These three models are built using coastal process modelling software, computational fluid dynamics (CFD) and Blade Element Momentum (BEM) codes. The disparate models are brought together into an Array Interaction Modelling (AIM) tool. In a world-first, the EnFAIT project provides an opportunity to validate this work at full scale, on a grid-connected array, with two rows of a total of six turbines spaced along and across the flow.

Presented in this paper is the work done toward developing an Array Interaction Modelling tool based on three separate codes. Also presented here is the full-scale field work being carried out to validate this model.

**Keywords**— ADCP, Array, Tidal, Turbulence, Wake

## I. INTRODUCTION

THE European Union Horizon 2020 funded project Enabling Future Arrays in Tidal (EnFAIT) carries out the demonstration of a grid connected tidal energy array. The aim of the EnFAIT project is to provide a step change in the life time cost of energy from tidal stream power. The project will deliver its targets by extending the existing Bluemull Sound tidal array from three to six devices. The six device array will achieve high availability and reliability through using best practice maintenance regimes.

The optimum tidal array delivers the greatest impact; be that energy generated, local community enrichment or valuable research outcomes. The six device array, in the EnFAIT project, will not only aim to demonstrate reliability but also maximise research contribution. In a world first, the turbine layout, within the array, will be adjusted throughout the project to enable array interactions to be studied and optimised.

Tidal streams offer predictable energy generation. A tidal stream is created by local geography channelling flow generated by the tide. Tidal streams are driven by lunar forces and generally governed by the principal lunar semi-diurnal constituent (M2) [1], or the time it takes the earth to rotate once relative to the moon. Nevertheless, local geography can have significant effects on the tidal flow. To extract the maximum benefit, from a tidal stream site, careful consideration of the tidal flow and local bathymetry is required.

The multi model approach set out in this paper is designed to model tidal turbine array interactions in a computationally practical yet physically accurate manner. The Array Interaction Modelling (AIM), which is carried out as part of the EnFAIT project, will inform the positioning of the tidal array installed in Bluemull Sound.

1654 - Tidal Hydrodynamic Modelling. This work was funded by the EU project EnFAIT, grant agreement 745862.

A. Macleod & S. Porteous are at Offshore Renewable Energy Catapult, Glasgow, UK, G1 1RD, (e-mail: [alsadair.macleod@ore.catapult.org.uk](mailto:alsadair.macleod@ore.catapult.org.uk), [sam.porteous@ore.catapult.org.uk](mailto:sam.porteous@ore.catapult.org.uk)).

D. Quantrell & A. Watson are at MetOceanWorks, London, E8 3DL, (email: [info@metoceanworks.com](mailto:info@metoceanworks.com)).

T. Wills is at Nova Innovation, Edinburgh, UK, EH6 6HQ (e-mail: [tom.wills@novainnovation.com](mailto:tom.wills@novainnovation.com)).

## II. THE ENFAIT SITE

The Nova Innovation EnFAIT tidal turbine array is located in Bluemull Sound. Bluemull Sound is between the islands of Yell and Unst in Shetland, Scotland. The tidal array is located just off the Cullivoe headland, Fig 1.

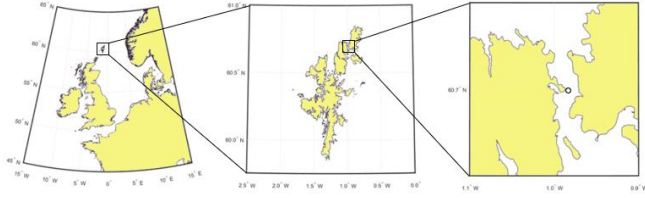


Fig 1. EnFAIT tidal array site location.

There are currently three turbines installed as part of the Bluemull Sound array. The array will be expanded to 6 turbines during the project. A detailed map of Bluemull Sound including depth contours is given in Fig 2. The three turbines are in a row, running from east to west, off the headland at Cullivoe, Fig 3.

Depth data, for Bluemull Sound, is available from several sources. Data has been taken from EMODnet, the UKHO INSPIRE portal, Oceanwise raster charts and a site bathymetric survey carried out on behalf of Nova Innovation. The regional coastline was discretised using the Global Self-consistent, Hierarchical, High-resolution Geography (GSHHG) Database.

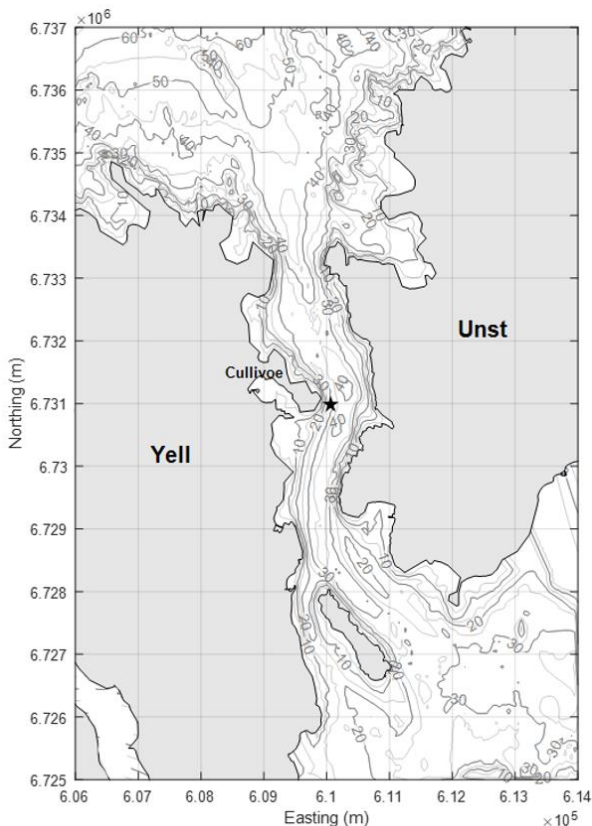


Fig 2. Bluemull Sound tidal site shown with bathymetric depth contours. The star indicates the tidal turbine site location.

Site recorded data has been used to seed and validate the models built as part of the EnFAIT project. Acoustic

Doppler Current Profilers (ADCPs) were installed concurrently across the turbine site to ensure good spatial resolution. The ADCPs were installed for a period of three months and recorded current data in 0.5m bins from 1.5m above the seabed to the water surface. The following campaign setups were used:

- **ADCP 1:** 10 minute average current readings *concurrent with* bursts of 850 current samples at 1Hz, starting every 30 mins.
- **ADCP 2:** same as ADCP 1.
- **ADCP 3:** 10 minute average current readings *concurrent with* bursts of 800 current and wave tracking samples at 1Hz, starting every 30 mins.

The ADCP locations are illustrated in Fig 3.

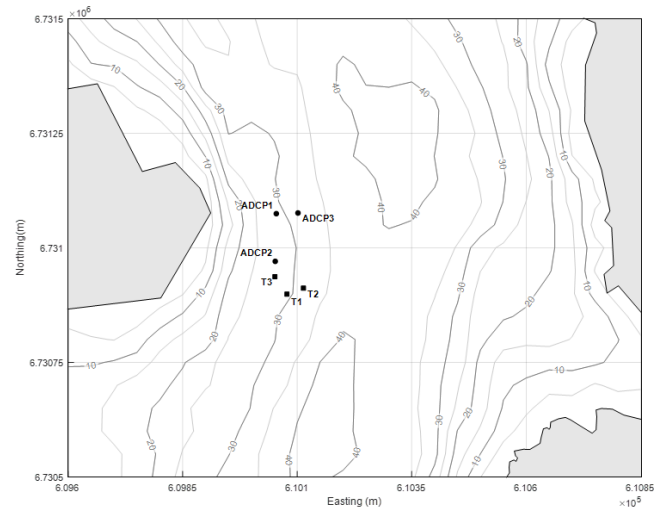


Fig 3. Locations of ADCP deployment and turbine locations overlaid on site bathymetry dept contours.

The 3 ADCP positions were selected to best understand the flow North of the existing 3 turbines (T1, T2 and T3). The flow to the North is of most interest as it is here the next 3 turbines, in the array, will be installed. The positions also give a good data spread across the consented site area.



Fig 4. Stainless steel ADCP seabed frames with bullseye.

The ADCPs were mounted in ballasted stainless steel frames, Fig 4. Using a multi-cat vessel, the frames were placed in the selected locations on the seabed. A spyball camera and frame mounted bullseye confirmed that the frames rested acceptably flat on the seabed, with a tilt of

less than 5 degrees. Ground lines and clump weights were used to further secure the frames in place and provided a method of recovery at the end of the deployment.

### III. AN OPERATIONAL BUT FLEXIBLE ARRAY

One of the greatest strengths of the EnFait project, in relation to array layout understanding, is the plan to restructure the array layout throughout the project duration. While final array positions are yet to be investigated, the high-level plan is to first install the turbines in a simple line array of three. This has been achieved and the turbines are operational with no wake effects impacting turbine performance.

Next, three further turbines will be installed to the north of the existing three turbines making an array of 6 turbines in two rows of three. The top two images, in Fig 5, show the initial six turbine array layout. The next three turbines will be installed approximately 20 diameters to the north of the existing three. This spacing will mean there is minimal array interaction between the rows of turbines. The flow around the turbines and the loading on the turbines will be recorded. This data will act as a benchmark which array interaction can be observed against.

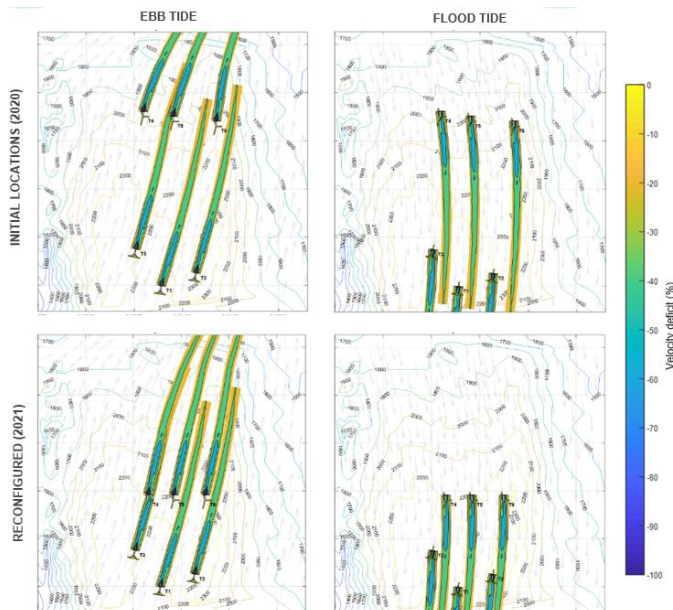


Fig 5. Turbine array layout showing wake velocity deficit contours.

Once data has been collected the array will be reconfigured. The streamwise spacing will be reduced to between five and ten diameters, the bottom two images, in Fig 5, show the stream wise spacing reduction planned. By targeting wake and turbine interaction on one of the devices, but aiming to avoid on the others, the project will directly measure the effect of array spacing and wake interactions. This data will be used to validate modelling work.

### IV. SITE DATA

The data, recorded by the site installed ADCPs, show complex flow behaviours. There is asymmetry between ebb (flow going from south to north) and flood (flow going from north to south) flow, there is complex wave and current interactions and there is a range of turbulence features displayed.

#### A. Site Flow

A sample of the recorded site flow data is represented in the tide rose show in Fig 6.

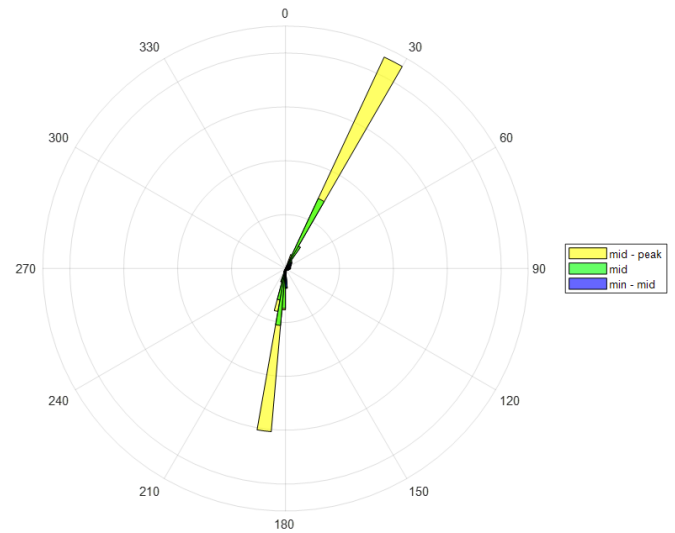


Fig 6. Site tide rose.

The tide rose shows the direction the tide is flowing to. In the recorded location (ADCP 1), the ebb tide flows at around 27 degrees from North. In flood the tide flows at around 187 degrees from north (to the South).

#### B. Shear profile

Shown, in Fig 7, are the recorded site flow velocity shear profiles. For comparison a power law profile [2] has been included.

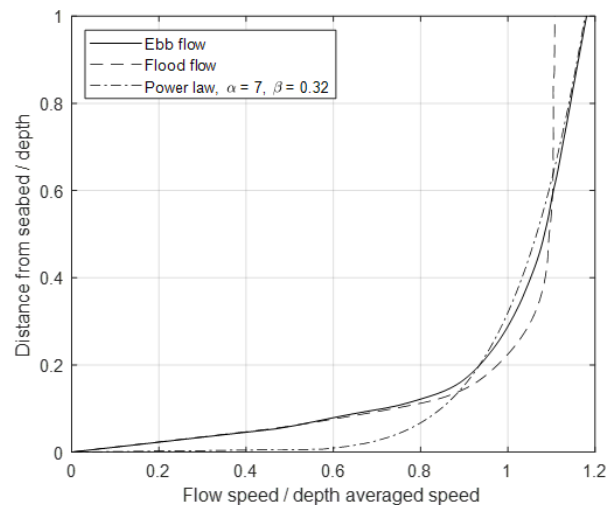


Fig 7. Site flow shear profiles for ebb, flood and a 7th power law.

The ebb profile shows continued flow speed increase towards the surface. This is inline with a typical power law governed profile. The flood profile, however, reaches peak



flow speed around the middle of the water column and this is maintained up to the surface. This asymmetry in current speed profile is due to the difference in route to site the flow takes in ebb and flood.

In ebb the flow is coming out of shallow water to the south and has longer to flow in the channel. These factors mean bottom friction is acting on the flow for longer allowing for the shear profile to develop. In flood the flow is coming out of deep water to the north, as a result, the shear profile does not have time to fully form.

### C. Wave Conditions

Wave conditions have been measured, on site, for a period of 3 months. From the measured data a range of wave conditions have been observed.

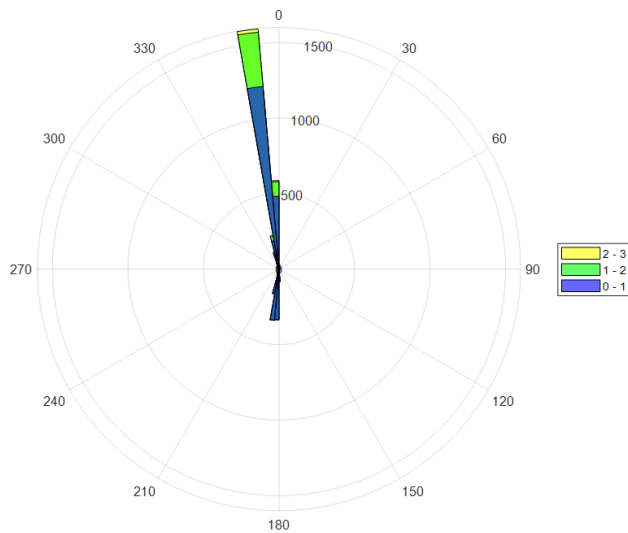


Fig 8. Site recorded wave direction. Wave direction is shown as coming from.

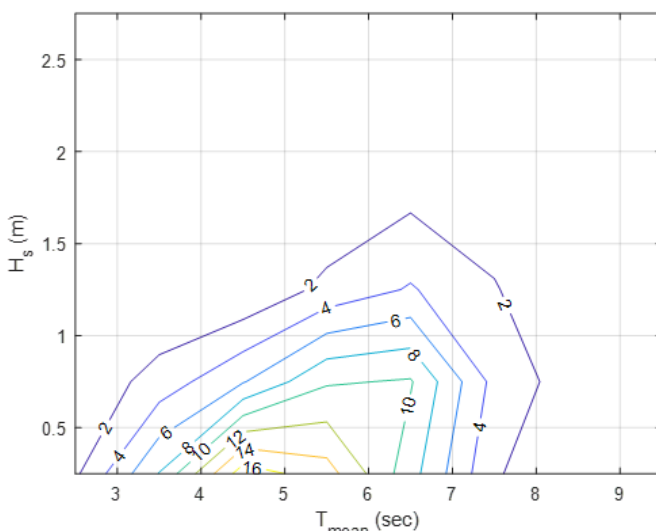


Fig 9. Site recorded wave climate occurrence map.

Wave direction is predominantly from the North with a little resource from the south. The site is very sheltered from waves in all other directions. The island of Linga to the south of the site helps to reduce the wave resource coming from the south. Only the north of the site is exposed to open ocean.

Looking at the occurrence map, Fig 9, it can be seen that, for the duration of the ADCP deployment, the majority of the wave resource is below 1 meter significant wave height. The wave resource mean period also tends to be short.

### D. Wave and current interaction

As stated, wave conditions on site are generally benign, the site is well sheltered from waves apart from those traveling from North. There is an observable difference in the waves coming from the north on an ebb to a flood tide, Fig 10.

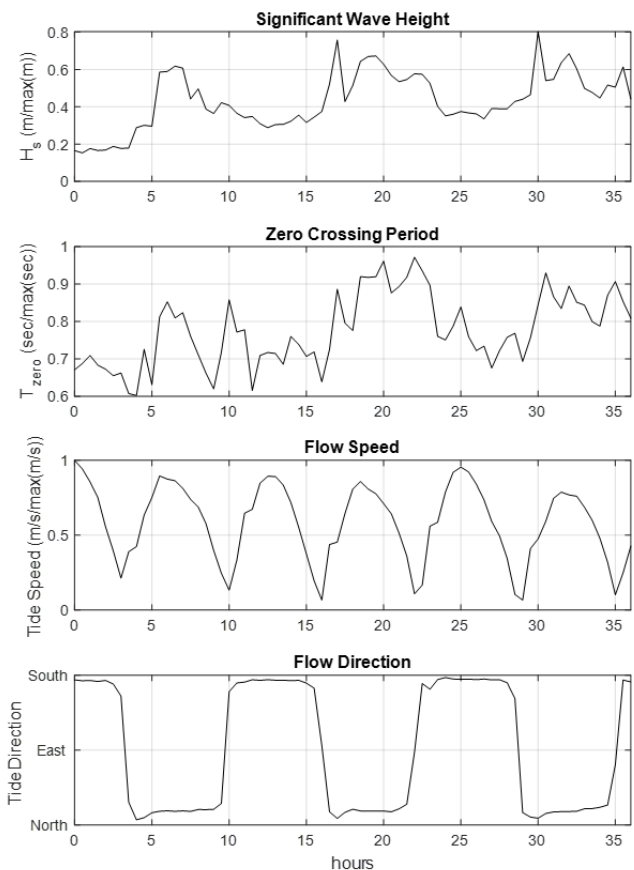


Fig 10. Plots showing 36 hours of concurrent wave and current data.

On an ebb tide, with the flow heading to the north and waves coming from the north (opposing wave and tide directions), wave heights tend to be larger and wave periods tend to be longer than on a flood tide.

There are several reasons for this, as waves enter the site from the north, and travel down the sound, the edges of the waves are slowed by the banks. This edge slowing tends to bow the waves with the centre traveling faster than the edges. The opposing tidal flow is fastest in the centre of the channel also, the action of the tide against the waves slows the centre of the wave train straightening the waves up. Straighter waves will penetrate further down the channel as they are less likely to bend into and break on the shores. As a result, more wave energy reaches the site.

The opposition of the tidal flow to the waves also tends to increase wave height; this can be observed in the data shown in Fig 10. This effect is comparable to waves shoaling in shallow water. Wave tidal opposition reduces wave group velocity, which is a reduction in energy transport speed. To maintain energy flux, with reduced transport speed, energy density must increase. An increased energy density is manifested by increased wave amplitude.

The waves recorded show a variation in spectral content depending on significant wave height and tidal flow direction. Considering the recorded wave spectra, Fig 12, it can be seen that on an Ebb or a Flood tide, with waves coming from the north (going south) and a significant wave height greater than two meters the wave spectra matches well to a theoretical JONSWAP spectra of matching peak period and significant wave height. As significant wave height is reduced the wave spectra becomes less peaky and more closely matches a Bretschneider spectra. With waves heading north, the available data shows good correlation with a JONSWAP spectra. Further work is required to understand the phenomena cause they observations.

#### E. Turbulence

Turbulence has been characterised by turbulence intensity. For a measured point in the velocity field, turbulence intensity,  $I_u$ , is defined as the root mean square of the time series velocity fluctuations,  $u'$ , divided by the mean velocity flow,  $\bar{u}$  [3].

$$I_u = \sqrt{\frac{\langle u'^2 \rangle - \text{noise}}{\bar{u}}} \quad (1)$$

Mean velocity flow has been taken over 10 minute intervals. Velocity fluctuations have also been taken over 10 minutes intervals, mean velocity fluctuations squared is defined by  $\langle u'^2 \rangle$ . Signal noise is removed to improve the estimate of turbulence intensity. For simplicity, in early analysis, noise has been defined as the square of velocity fluctuations ( $\langle u'^2 \rangle$ ) at slack tide.

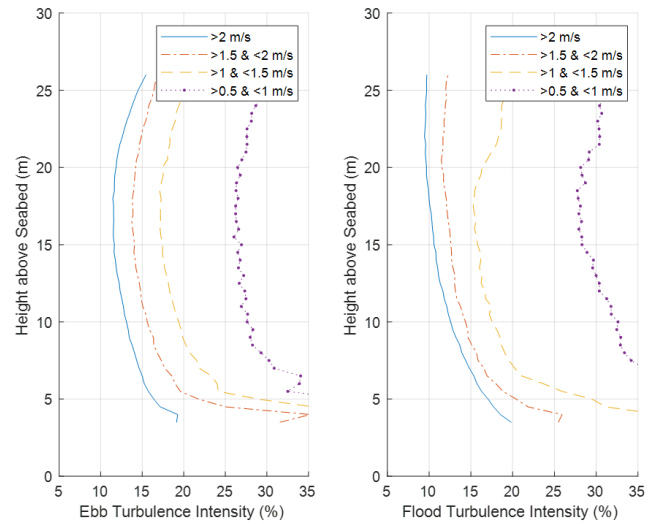


Fig 11. Site turbulence intensity.

Turbulence intensity has been found through the water column, for ebb and flood flow, at a range of hub height flow speeds. Note that there is an increase in turbulence intensity with decreasing flow speed. As turbulence intensity is calculated with velocity as the denominator, a similar level of velocity fluctuation will have a larger turbulence intensity at a lower flow speed.

From the analysis performed, it can be seen that in operational flow speeds (generally considered to be  $>1\text{m/s}$ ) turbulence intensity varies from around 12 to 20%. Measured turbulence intensity values will be used to build and calibrate wake numerical models.

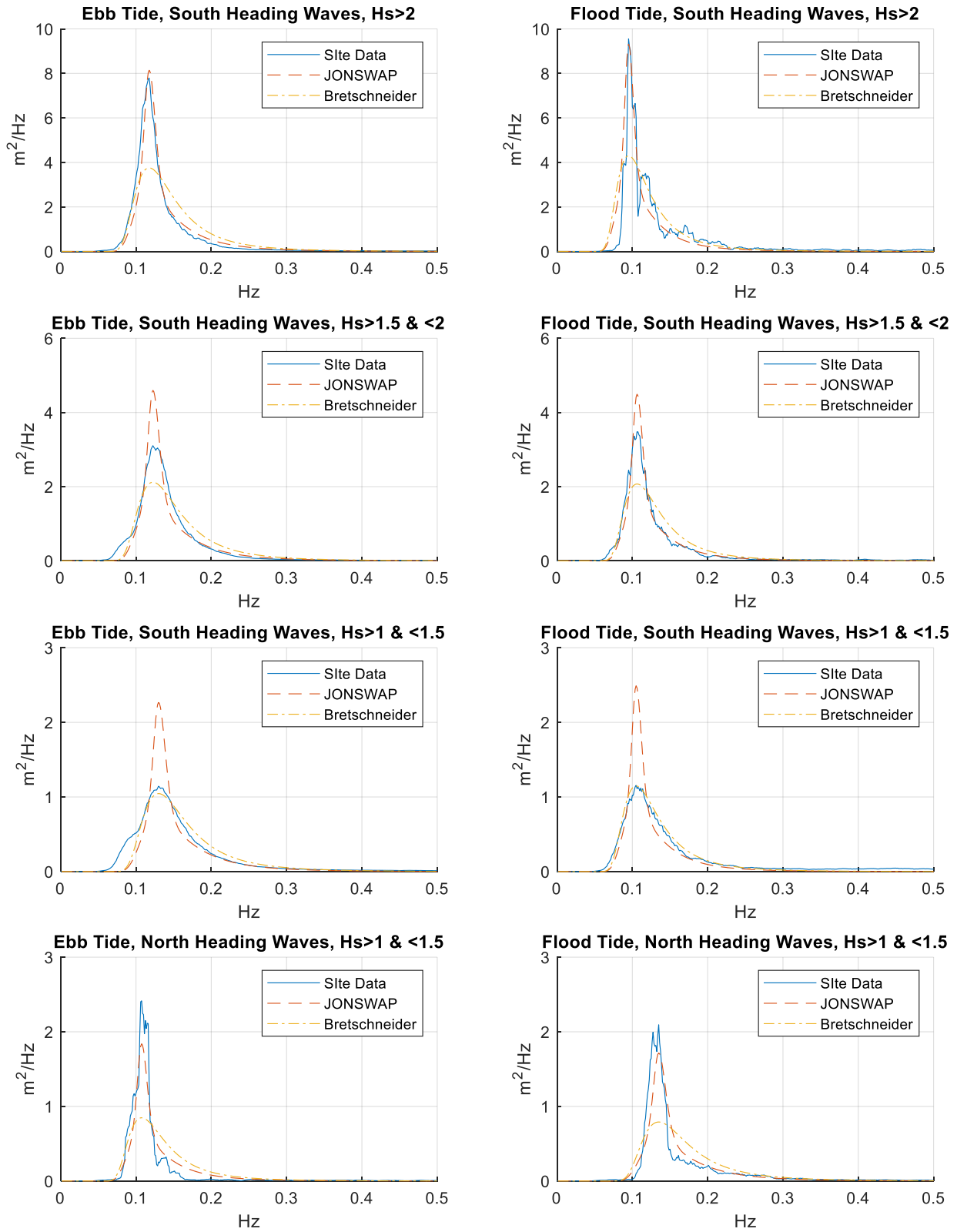


Fig 12. Wave spectra for various combinations of tide and wave direction and significant wave height.

## V. MODELLING APPROACH

The array modelling technique presented is based around 3 modelling methods, a site resource model, a wake model built using Computational Fluid Dynamics (CFD) and a Blade Element Momentum (BEM) model. The results from these three models are brought together in MATLAB to produce a tool to inform array design.

The modelling approach has been selected to offer a balance between complexity and computational efficiency. The tool to be created aims to be physically accurate, and useful for modelling array loading and power effects, while remaining practical to execute. The approach is semi empirical and is built upon high fidelity site and turbine data and numerical simulations.

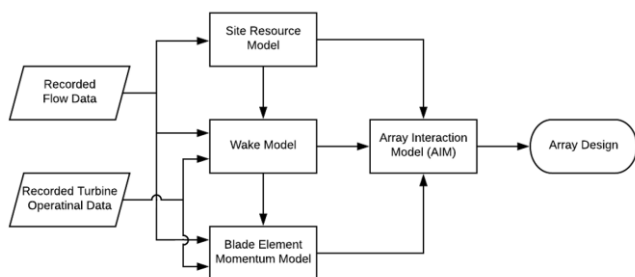


Fig 13. Modelling approach flow diagram.

The array interaction model will be built around 3 detailed numerical models, site flow data and turbine data. A flow diagram illustrating the modelling approach is shown in Fig 13.

### F. Site Resource Model

Of the three models which underpin the AIM tool, the site resource model is the only one complete and validated. The site resource model includes modelling of both hydrodynamics and waves. Due to complexity in accurately representing wave and current interaction the hydrodynamic and wave components of the resource model are uncoupled. Both aspects of the resource model have been validated using site installed ADCPs. The hydrodynamics show very good correlation with recorded data, the wave model less so.

### G. Hydrodynamic Model

For the hydrodynamic model current and water level parameters were produced using a European, basin-scale flexible mesh hydrodynamic model. The underlying model has been developed using the MIKE21 2D modelling package, a comprehensive modelling system for two-dimensional water modelling developed at the Danish Hydraulic Institute (DHI).

For this project, additional resolution was incorporated into the model around the project area. In total, the model consisted of 223,215 triangular tessellations, the majority of which were in the Shetland area, where maximum horizontal resolutions of between 15-20m were achieved in Bluemull Sound.

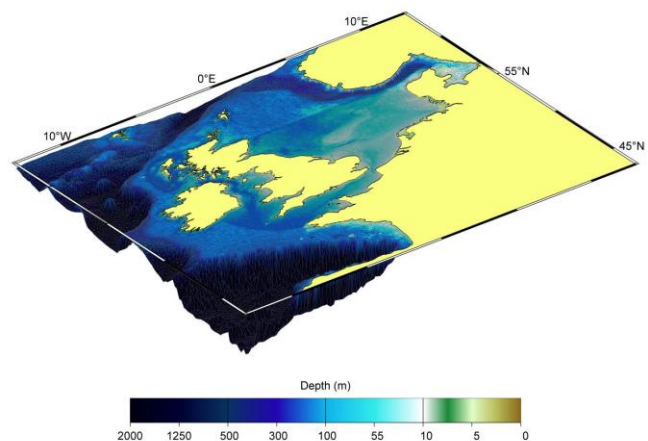


Fig 14. Regional European MIKE21 flexible model mesh.

Tidal boundary conditions originated from the TPXO 7.2 Atlantic Ocean model. Maintained by the Oregon State University, TPXO7.2 is the latest version of a global model of ocean tides, which best-fits, in a least-squares sense, the Laplace Tidal Equations and along track averaged data from the TOPEX/Poseidon and Jason satellites.

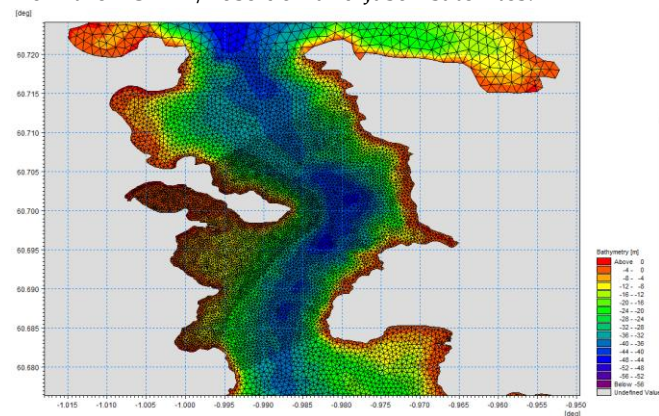


Fig 15. Local MIKE21 flexible model mesh.

The hydrodynamic model was calibrated against water levels and velocities measured from ADCP measurements. The three ADCPs were installed for the period 15/09/2001 to 17/10/2001. The three ADCPs locations are shown in Fig 3 and the equivalent locations are: 60°42.007'N & 0°59.037'W (for site A), 60°41.951'N & 0°59.043'W (for site B) and 60°42.007'N & 0°59.037'W (for site C).

Modelled water levels from the hydrodynamic model are compared with measurements at the three ADCP locations.



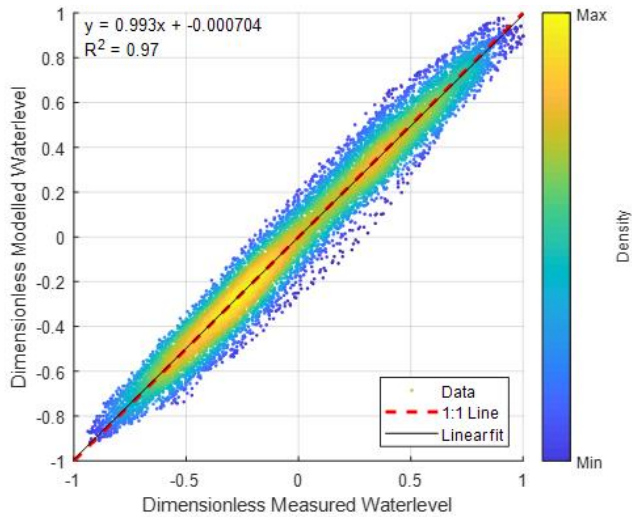


Fig 16. Water Level comparison at ADCP 1.

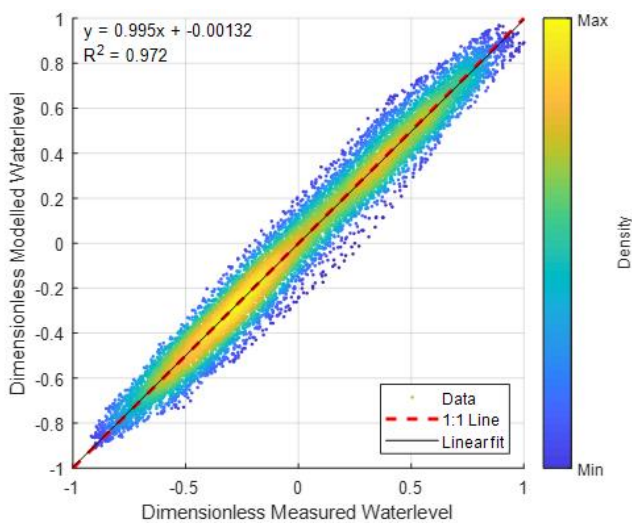


Fig 17. Water Level comparison at ADCP 2.

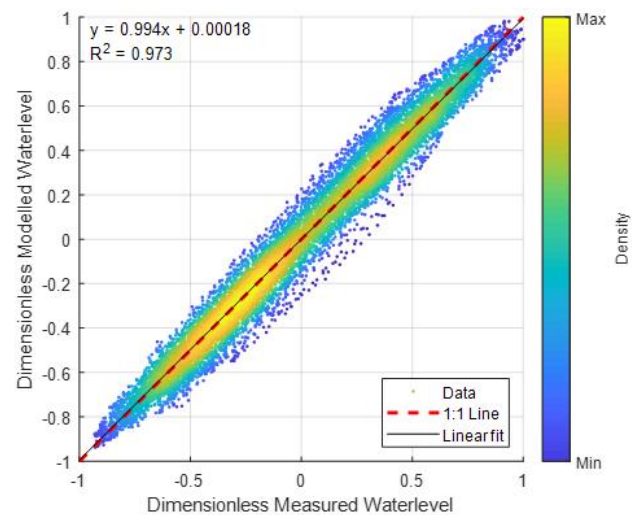


Fig 18. Water Level comparison at ADCP 3.

A good correlation can be seen across all three deployed ADCPs, Fig 16, Fig 17 and Fig 18.

## H. Wave Model

A high resolution (9km) European Shelf wave model which has been run to produce a 39 year European wave hindcast, developed by MetOceanWorks, provided boundary conditions to a high resolution nested wave model local to the Shetland Islands and Bluemull Sound for the 20 year period from 1998 to 2017. The deployment of a high resolution nested wave model that properly accounts for shallow water processes is necessary to account for the complex regional bathymetry and coastline which affects the evolution of the local wave climate. The Shetland area model had a regularly spaced grid with a horizontal resolution of 1km whilst the final nest of Bluemull Sound was unstructured and had a maximum horizontal resolution of 60m in the vicinity of the study area.

The underlying wave models have been developed using SWAN (Simulating WAVes Nearshore), a third-generation wave model, developed at Delft University of Technology (TU Delft), which computes random, short-crested wind-generated waves in coastal regions and inland waters. SWAN accounts for the following physics:

- Wave propagation in time and space, shoaling, refraction due to current and depth, frequency shifting due to currents and non-stationary depth.
- Wave generation by wind.
- Three- and four-wave interactions.
- Whitecapping, bottom friction and depth-induced breaking.
- Wave-induced set-up.
- Transmission through and reflection (specular and diffuse) against obstacles.
- Diffraction.

For the production run, SWAN cycle III version 41.20 was used and employed the expression by Komen for white capping and for wind. Triads were included and quadruplet interactions were estimated using the Discrete Interaction Approximation (DIA) by Hasselmann. The JONSWAP bottom friction formulation was used and depth-limited wave breaking was modelled according to the bore-model of Battjes and Janssen.

Significant efforts were made to include hydrodynamics in the unstructured nested wave model of Bluemull Sound. However, the study area is so complex in terms of wave/current interactions that it ultimately proved too expensive both in terms of time and computational effort to achieve good calibration. As a result, the final wave model did not include hydrodynamics.

Comparisons of measured and modelled waves (without currents) are given in Fig 19 and Fig 20. These plots demonstrate that the wave model without currents sufficiently describes the mean wave behaviour.



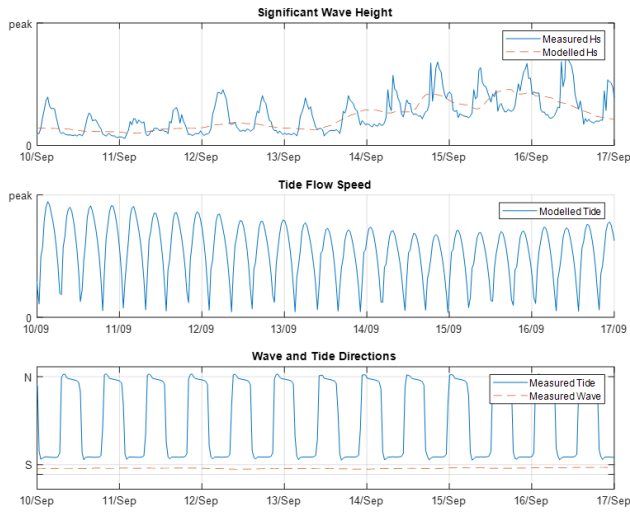


Fig 19. Time series of measured and modelled waves.

It can also be seen, from these plots, that there is a significant relationship between tide speed, tide direction wave direction and whether Hs is under or over predicted, Fig 19.

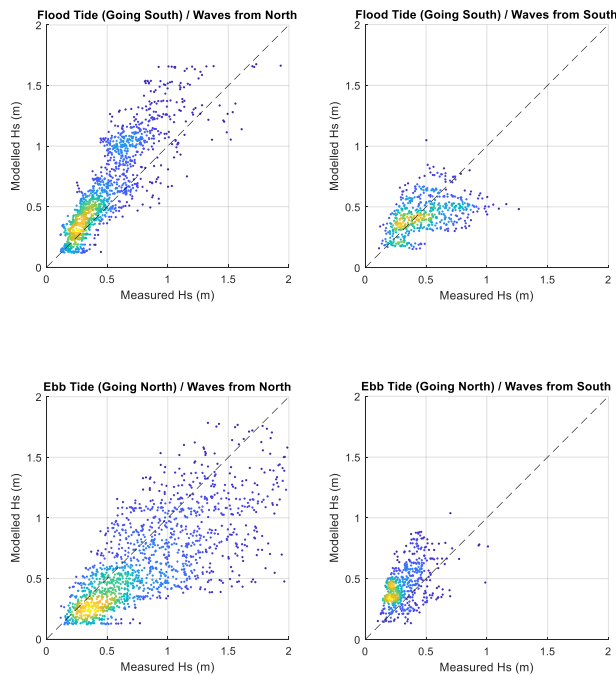


Fig 20. Comparison of measured and modelled Hs, plot coloured to show scatter density.

Looking in more detail at the comparison of predicted Hs to measured we can start to see how the tide is altering the wave climate. For the case of the tide running in flood (from north to south) and waves coming from the north it can be seen that Hs tends to be over predicted. When the tide and the waves are running in the same direction Hs is reduced from predicted.

The opposite can be seen with the tide flowing in ebb (from South to North) and the waves coming from the south, Fig 20. The model tends to under predict wave height. When the tide and the waves are running in opposite directions Hs is increased from predicted. There

is less data available when waves arrive at site from the south. This is due to the site geography. The relationships established are less obvious but still apparent.

Looking in more detail at Ebb tides with opposing waves from the north, Fig 21, it can be seen that there is a relationship between tide speed and the prediction of Hs. The model under predicts Hs to a greater extent with greater flow speed. It can also be seen that at the lowest flow speeds the model over estimates Hs.

The complex relationship between flow speed, flow direction, wave direct and wave height makes prediction of wave induced flow velocity fluctuations at the turbine difficult. Further research needs to be performed to properly inform future array load modelling.

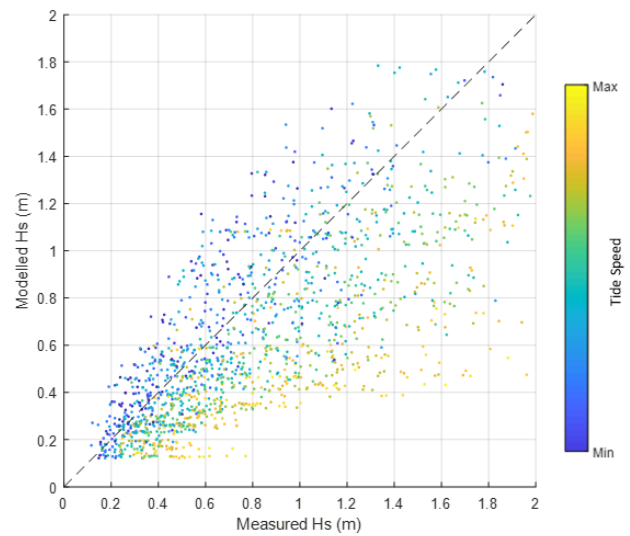


Fig 21. Comparison of measured and modelled Hs on an Ebb tide with waves from the north, plot coloured by tide flow speed.

### I. Wake Model

A detailed review of wake modelling techniques has been carried out in the paper *Review of tidal turbine wake modelling methods — state of the art* by E.Jump [4]. This has informed the modelling decisions taken on the EnFait project.

Accuracy in wake models is required 3 blade diameters and more away from the turbines for good array interaction understanding. The wake immediately behind the turbine does not need to be accurately represented to understand how it impacts a turbine further downstream.

Velocity defecate, turbulence and swirl are all wake features which will impact array design. Detailed models have been built in using RANS CFD. These have been calibrated using site recorded flow data and represent velocity defecate well at greater than five diameters downstream. Accurate representation of swirl and turbulence is yet to be demonstrated.

The EnFait project will tackle array modelling with regards to wakes and turbulence in 2 ways. The first is an 'good enough' approach. This approach aims to model the wakes and turbulence to a fidelity that allows an array to be designed with confidence the turbines are in

appropriate if not perfect locations. Then through site measurement improve and refine the modelled estimates.

Rather than try to model all site phenomena perfectly, basic numerical models will be tuned to represent the conditions measured on site. The motivation behind this approach is to reduce computational overhead but maintain tool usefulness.

Alongside this approach a full array model will be built. This model will employ a large-eddy simulation-actuator line method (LES-ALM). The model will be applied to the site and validated against measured site data. The LES-ALM is capable of capturing complex wake dynamics, including tip vortices. The LES-ALM will be employed to replicate the wake behind the turbines in the array while including a geometric representation of the local site bathymetry.

A comparison of the 2 modelling methods will be made against each other and against site recorded data. This comparison will allow for a quantifiable measure of accuracy to be made helping to inform the effort required to represent wakes and array interactions well.

#### J. Blade Element Moment Model

In conjunction with the RANS CFD wake model, a turbine Blade Element Momentum (BEM) model will be built. This model will be run using flow inputs generated from site recorded data and model results. The model will be run for a range of conditions, including variations in flow speed, turbulence characteristics and wake representations. These results will be used to estimate long-term site performance in various array configurations.

#### K. Array Interaction Model (AIM)

The site flow models, wake CFD models and turbine BEM model shall be combined to produce an Array Interaction Model (AIM). The AIM will be a tool that allows quick and computationally cheap site assessment. Using a semi-empirical approach, based on the 3 models run and validated by site recorded data, the tool will assess array designs for performance and loading.

The tool, while not modelling complex flow physics, will be robust and fast. It will allow multiple array designs to be assessed. The AIM tool will be validated against site recorded data and the complex LES-ALM model. The LES-ALM model will run a reduced number of array designs as proof cases.

#### ACKNOWLEDGEMENT

A. M. thanks R. Flatman and P. Wilson of Partrac Ltd for their support and advice in ADCP deployment.

A. M. thanks O. Bethwaite and crew for their support in ADCP deployment.

#### REFERENCES

- [1] D. Pugh, P. Woodworth, and B. Parker, *Tidal analysis and prediction*. 2007.
- [2] M. Lewis, S. P. Neill, P. Robins, M. R. Hashemi, and S. Ward, "Characteristics of the velocity profile at tidal-stream energy sites," *Renew. Energy*, vol. 114, pp. 258–272, Dec. 2017.
- [3] D. R. J. Sutherland, B. G. Sellar, V. Venugopal, and A. G. L. Borthwick, "Effects of Spatial Variation and Surface Waves on Tidal Site Characterisation," *Proc. 12th Eur. Wave Tidal Energy Conf.*, pp. 1–8, 2017.
- [4] E. Jump, A. Macleod, and T. Wills, "Review of tidal turbine wake modelling methods — state of the art."